Honors College Theses

4-26-2022

Investigating Ionic Current Rectification as a Means of Controllable Drug Delivery using Silica Nanoparticles and Nano Porous Membranes

Katie L. Nolan
Georgia Southern University

Investigating Ionic Current Rectification as a Means of Controllable Drug Delivery using Silica Nanoparticles and Nano Porous Membranes

An Honors Thesis submitted in partial fulfillment of the requirements for Honors in Chemistry

By Katie Nolan

Under the mentorship of Dr. Ji Wu

<u>Abstract</u>

This project investigates a novel ionic current rectification (ICR) phenomenon created by the opening and closing of nanopores by charged silica nanoparticles (SNPs) under electrophoretic flow. This voltage-controlled opening and closing of the pores can be exploited to allow delivery of nicotine through the pores at programmable intervals. The ICR phenomenon was thoroughly investigated by varying pH, buffer concentration, SNP concentration, and applied voltage range. The mechanism was also verified by testing with a 2-, 3-, and 5-electrode system. Potential cake layer formation was demonstrated in a longer ICR test, and the implications of this on the drug delivery mechanism were discussed.

Thesis Mentor: _____

Dr. Ji Wu

Honors Director: _____

Dr. Steven Engel

April 2022
Department of Chemistry and Biochemistry
Honors College
Georgia Southern University

<u>Acknowledgements</u>

I would like to thank:

My mentor, Dr. Ji Wu for his continued support and advice

Lab mates Jennifer Iwenofu, Jake DiCesare, Juan Mitchell for their assistance and contributions to the project

The Georgia Southern University Department of Chemistry and Biochemistry for their facilities and support from the faculty

The Georgia Southern University Honors College for funding this opportunity

Table of Contents

Introduction

Nanochemistry in Medicine. Nanomaterials of various types are being widely investigated and used to develop efficient drug delivery systems. Silica nanoparticles (SNPs) for example, have strong potential due to ease of surface chemistry modifications and nanopores of various sizes that make them ideal *in-vivo* drug carriers.[1] These types of mechanisms, also seen in studies using nanotubes and nanofibers, often respond to cell environment stimuli like pH, redox, and enzymes, or to outer stimuli such as temperature, ultrasound, and magnetic field.[2–4] Beyond body chemistry, the rates of delivery in devices such as hormone implants, long-term therapy for HIV patients[5], and treatments for opioid addiction[6] rely on passive release of the drug over time. While useful in some circumstances, it is desirable to be able to wirelessly vary dosage amounts independent of body chemistry. This is particularly true in patients needing a pain management device or for addiction treatment. The mechanism needs to be controllable, meaning that the dose can be varied, and ideally also programmable, to release a drug at a predetermined time or over certain intervals. Keeping these qualities in mind, this study aims to develop a nanoporous system gated by SNPs, as opposed to using them as drug carriers.

Ionic Current Rectification (ICR). Ionic current rectification (ICR) is a relatively new electrochemical phenomenon created by nanopores experiencing some type of asymmetry in shape or charge or both.[7] Nanopores that exhibit ICR can be designed to be permanently structurally asymmetric, a conical pore for example, or a structurally cylindrical pore can be manipulated by an external force, such as pressure or deposition, to produce deformations that break the symmetry.[8,9] Charged molecules can be deposited on to the inner walls of a pore or the outer surface of a many-pore membrane to create charge asymmetry.[10,11] This means ICR is often

sensitive to changes in pH and buffer concentration, allowing one to manipulate the extent of the rectification.[7] This mechanism is governed by the Poisson-Nernst-Planck equations, which includes variables such as wall surface charge, electrolyte concentrations and diffusion coefficients, pore diameter, effective length, and many more.[7]

Hypothesis. This study provides a unique use for SNPs in demonstrating the ICR phenomenon through track-etched polycarbonate nanoporous membranes. These membrane pores are cylindrical and inert, unlike the ICR systems described above. Instead, we hypothesize that ICR can be created by electrophoretic migration patterns of charged SNPs in an electric field. Two solutions, each containing oppositely charged SNPs, are separated by a membrane. When potential differences of opposite polarities are applied across the membrane, migration of particles should result in a blocking and unblocking of the pores, assuming that the particles are larger than the nanopores. Blocking of pores will hinder the passing of electrical current across the membrane, while unblocking of pores will allow current to freely flow. This describes the characteristic ICR curve produced in other studies. Naturally, the blocking and blocking of the nanopores can prevent and allow the passive diffusion of a drug through the pores depending on the polarity of voltage applied. This effect has been thoroughly investigated in our lab. Parameters tested include variations in pore size, particle size, pH and concentration of buffers, magnitude of voltage applied, and distance between electrodes. Each parameter has been optimized before applying the mechanism to diffusion of small drug molecules like nicotine. This ICR system will be programmable and effectively provide more accurate and timely dosage patterns for use in drug addiction and abuse treatments.

Materials and Instrumentation

Nucleopore Track-Etch 0.015 µm membranes were purchased from Whatman. Ag/AgCl 0.015" diameter electrodes were obtained from A-M Systems and a Sigma Aldrich Ag/AgCl reference electrode was used. Tetraethyl orthosilicate 98% from Acros Organics was used and 3-Aminopropyltriethoxysilane 98% and (S)-Nicotine (99%) were obtained from Alfa Aesar. ACS grade ammonium hydroxide 28-30% was purchased from VWR Analytical, as was the HPLC super gradient acetonitrile and syringe filters (13nm) with 0.2 µm PTFE membrane. Disposable syringes (1 mL) without needles were bought from Air-Tite Products and Co. HPLC grade sub-micron filtered water by Fisher Chemical was used.

The HPLC instrument used was from Shimadzu: LC-20AT, DGU-20A 5R degassing unit, SIL-20A HT autosampler, SPD-20A UV/Vis detector, CBM-20A communications bus module. A HyPurity C18 reverse phase HPLC column was purchased from Thermo Scientific, with specifications of 250 x 4 mm and particle size 5 µm. A Malvern Nano-ZS90 Zetasizer was used to test the surface charge and size of the synthesized SNPs using dynamic light scattering (DLS). Pore sizes of the nucleopore Track-Etch 0.015 µm Whatman membranes were confirmed using a field emission scanning electron microscope: JEOL JSM-6620 LV. The ICP-MS instrument used in the Fick's Law experiment was the ICP-MS NexION 300X by Perkin Elmer.

Experimental

Silica nanoparticle synthesis. Silica nanoparticles were synthesized using the well-established Stöber method for 8 hours, targeting particles with a diameter of 50 nm.[12] All SNPs were centrifuged at 7,500 rpm for 20 minutes, 3 times each with 5-minute breaks between. Liquid

was poured off and the SNP pellet immediately redispersed in ethanol by vortexing followed with

20 minutes of sonication. 3-Aminopropyltriethoxysilane (APTES) was added to this cleaned SNP

solution for functionalization. The reaction was sonicated as it ran for 15 minutes. The same

centrifugation conditions were used for the functionalized SNPs, but only for 2 cycles, and the

pellet was immediately redispersed under the same conditions. All final SNP solutions had a

concentration of 1% (w/v). Functionalized and non-functionalized nanoparticles were dispersed in

0.01 M pH 3 citrate and 0.01 M pH 10 phosphate buffers respectively and vortexed for 30 seconds

each before size and zeta potential measurements.
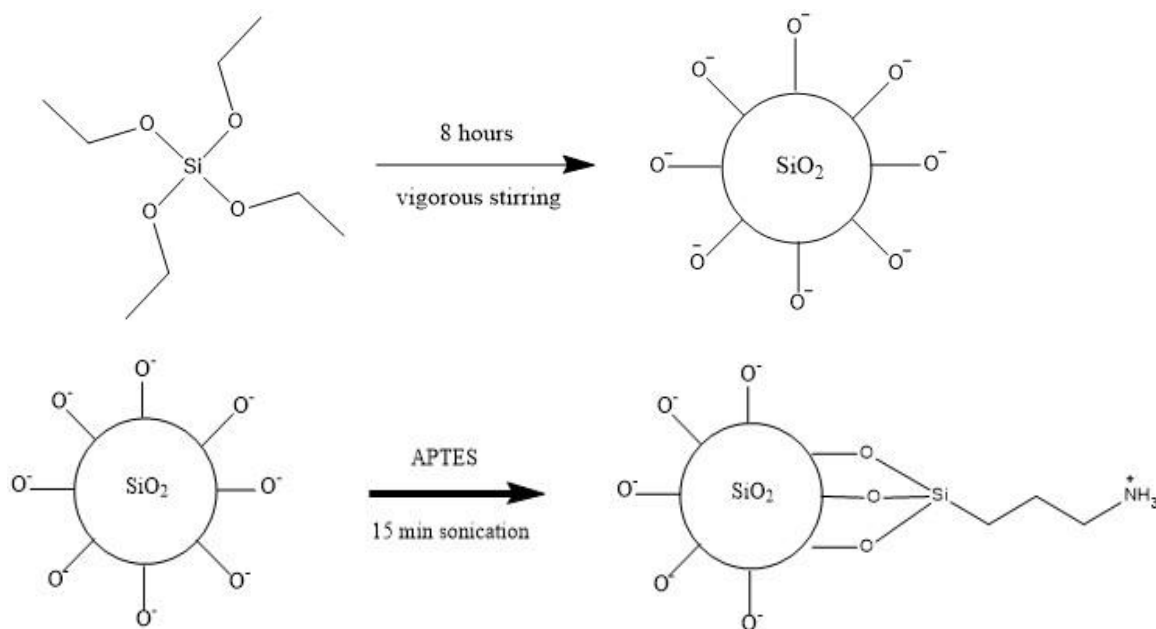
Figure 1. Self-assembly of SNPs using the Stöber method and the functionalization reaction.

Membrane fabrication. Duct tape was cut into approx. 1-inch squares and the center of

each piece was punctured with an Air-Tite disposable needle. A Whatman 15 nm nano porous

membrane was placed over the puncture on the sticky side of one piece of duct tape. The other

piece of duct tape was laid over the top with the punctures aligned and the membrane between. A

ring of Gorilla Glue epoxy was used to surround but not cover the puncture on one side of the final

membrane structure only, shown in Figure 2. The puncture area was checked under a microscope to ensure it was not blocked with epoxy. This design was reproducible for the purposes of this research project but needs further development for future applications.
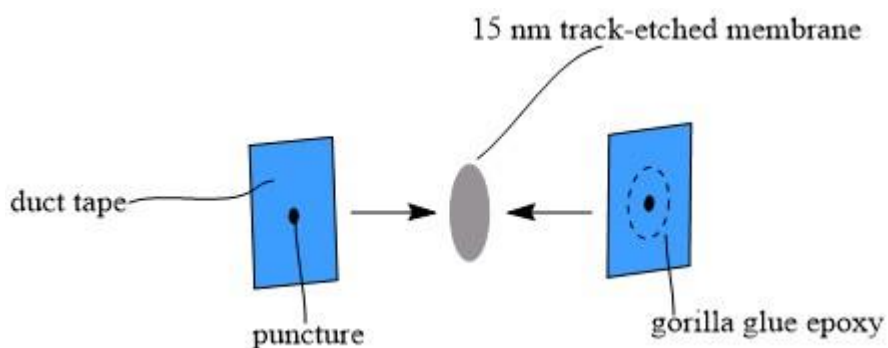

Figure 2. Fabrication of membranes. Note: Duct tape is represented by the blue shaded area.

Membrane efficacy. The efficacy of a membrane to produce ICR had to be tested before being applied to drug trials. Most parameters used in these tests were determined by the previous research of Chris Pintro[13], where he optimized on/off ratios. Using a U-tube setup, 300 μL of 1% (w/v) functionalized SNPs were added to 0.01 M pH 3 citrate buffer and 300 μL of 1% (w/v) non-functionalized SNPs were added to 0.01 M pH 10 phosphate buffer. Each side of the tube was brought to a final volume of 6 mL. The working electrode was placed in the pH 3 solution and the counter electrode and reference electrode in the pH 10 solution. A voltage window of -0.6 V and +0.6 V was applied for 3 cycles of approximately 4 minutes each.

An important numerical measure of efficacy for membranes in these ICR tests was the calculation of an on/off ratio. Previous research determined that this ratio must be >3 for membranes to be considered efficient.[13] This is calculated by dividing the current at the most negative voltage by the current at the most positive voltage, and taking the absolute value of the

answer. Only the most efficient were used in drug diffusion studies, averaging an on/off ratio of 11.36.
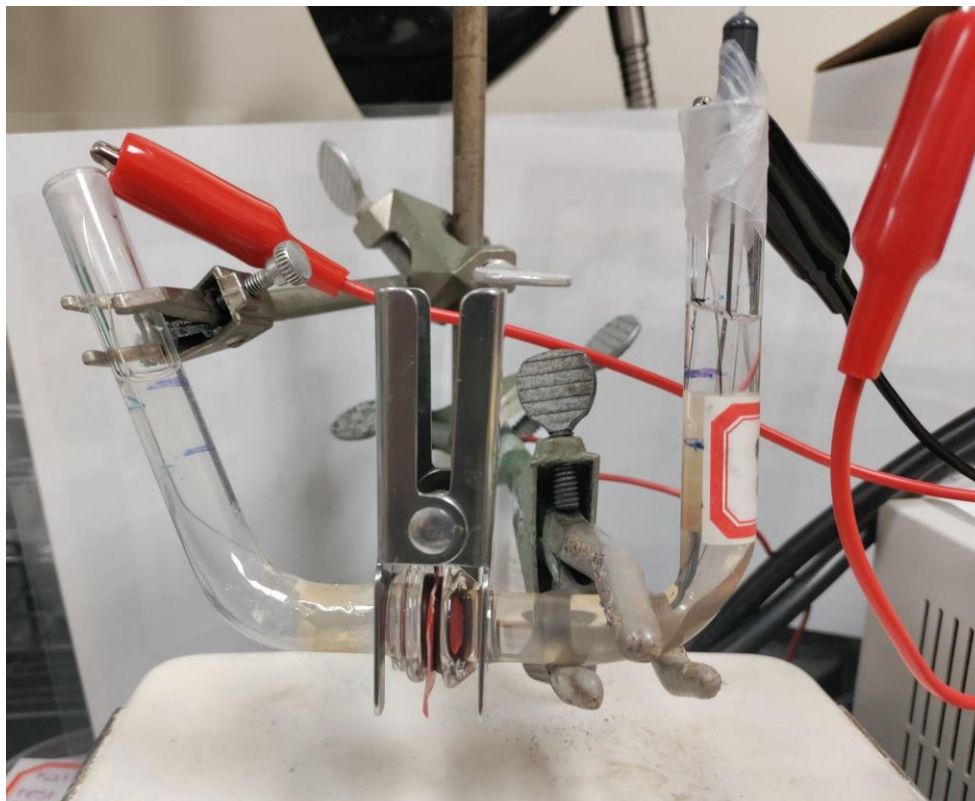
Figure 3. The experimental setup of a 3-electrode electrochemical cell for ICR tests. The left shows the pH 3 solution containing the working electrode. The right shows the pH 10 solution containing the counter electrode (black) and the reference electrode (red).

Proof of ICR Concept. To complement the use of a 3-electrode system, tests were also done using a 2-electrode system containing working and counter electrodes only and a 5-electrode system, which included adding a sensor electrode to each side of the setup. A test of 30 cycles of alternating -0.6 to +0.6 V was done continuously using the 3-electrode system to assess the possibility of gradual formation of a "cake layer" of nanoparticles on the surface of the membrane.

Fick's Law of Diffusion. Fick's law was used to determine the diffusion coefficient for nicotine and thereby the optimum donor concentrations and diffusion time. The U-tube was set up with a 1000 ppm KCl donor solution on the left and deionized water on the right. A reliable membrane of on/off ratio ∼22 was used. The setup was left to diffuse passively for 4 hours, after which the diffusion side was separated into two samples and diluted. Inductively Coupled Plasma Mass Spectroscopy (ICP-MS) was used to create an internal standard curve of known KCl concentrations, and the unknown concentration of the diffused solution was calculated from this. After a series of calculations, it was determined that a donor concentration of 10,000 - 15,000 ppm was needed to be comfortably above the limit of detection (LOD) and limit of quantification (LOQ) of the HPLC quantification method for nicotine.

Nicotine delivery using the ICR system. For nicotine diffusion trials, voltages of -0.6 V, and +0.6 V were run for 24 hours each for a total test time of 48 hours. These diffusion trials used the 2-electrode system and small stir bars were added to each tube for the duration of these tests. The pH 10 solution is the nicotine donor for the system, to which 80 μL of pure nicotine was added. To measure diffusion over time, 1 mL aliquots were removed from the pH 3 buffer at hours 8, 25, 32, and 48. Volume was kept constant by replacing volume taken with fresh pH 3 buffer. Each sample was filtered using an Air-Tite 1 mL disposable syringe and a VWR 13 nm filter before being transferred to the HPLC vials. Samples were analyzed by reversed-phase high performance liquid chromatography (RP-HPLC) using the conditions shown in Table 1.[14]

Column information	C18; 250 x 4 mm
Mobile phase A (70%)	0.1% triethylamine in water at pH 11
Mobile phase B (30%)	acetonitrile
Flow rate	1.00 mL/min
Run time	7 minutes
Detection wavelength	254 nm

Table 1. HPLC parameters.

Samples were analyzed using the Shimadzu HPLC system and Lab Solutions software. Under the conditions stated in Table 1, nicotine eluted around 4.7 minutes. Triplicate analysis of each set of diffusion trial samples was performed. An external standard calibration method was used. Standards were made using a stock solution of 1000 ppm nicotine in DI water and were further diluted with DI water where needed.

Results

SNP and Nanoporous Membrane Characterizations
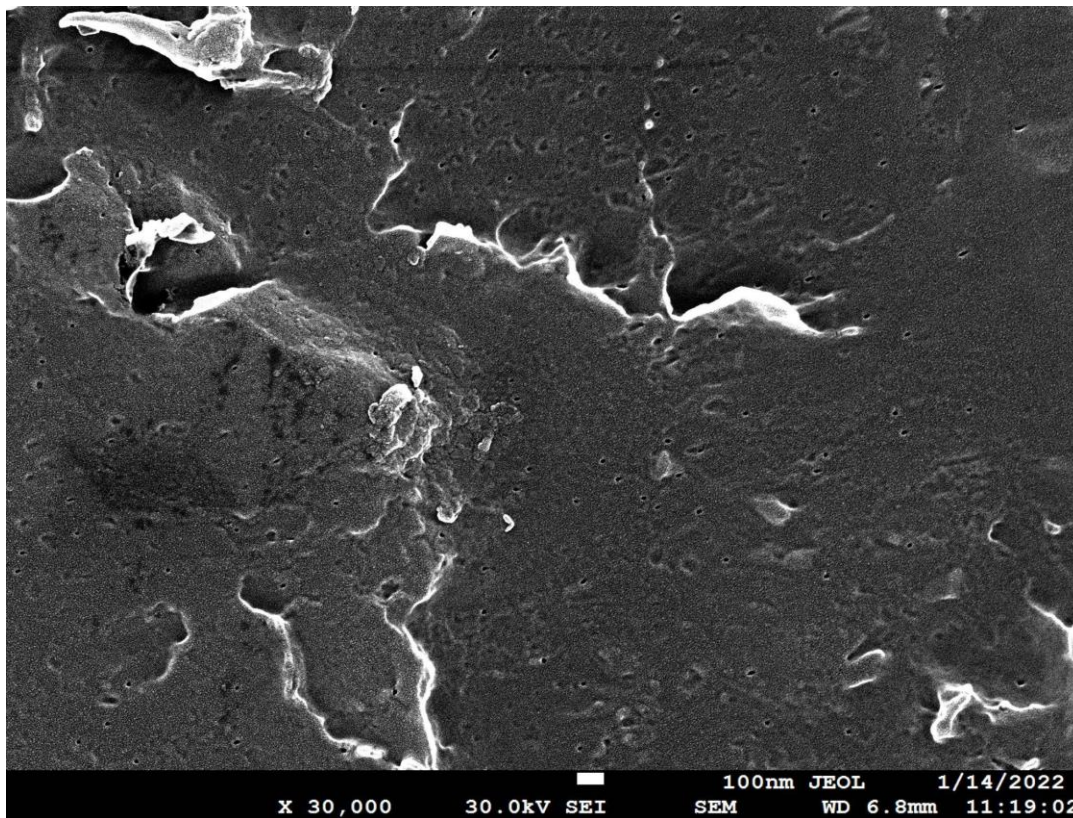
Figure 4. SEM image of a piece of track-etched polycarbonate membrane with 15 nm pores used

in this study.

Non-Functionalized SNPS				Functionalized SNPs			
Diameter (nm)	%RSD (nm)	Zeta (mV)	%RSD (mV)	Diameter (nm)	%RSD (nm)	Zeta (mV)	%RSD (mV)
72.38	1.1	-14.1	13.1	187.0	3.8	+35.0	1.25

Table 2. Summary of size and zeta potential (surface charge) characterizations of SNPs using

DLS on a Malvern Zetasizer.

ICR Proof of Concept.
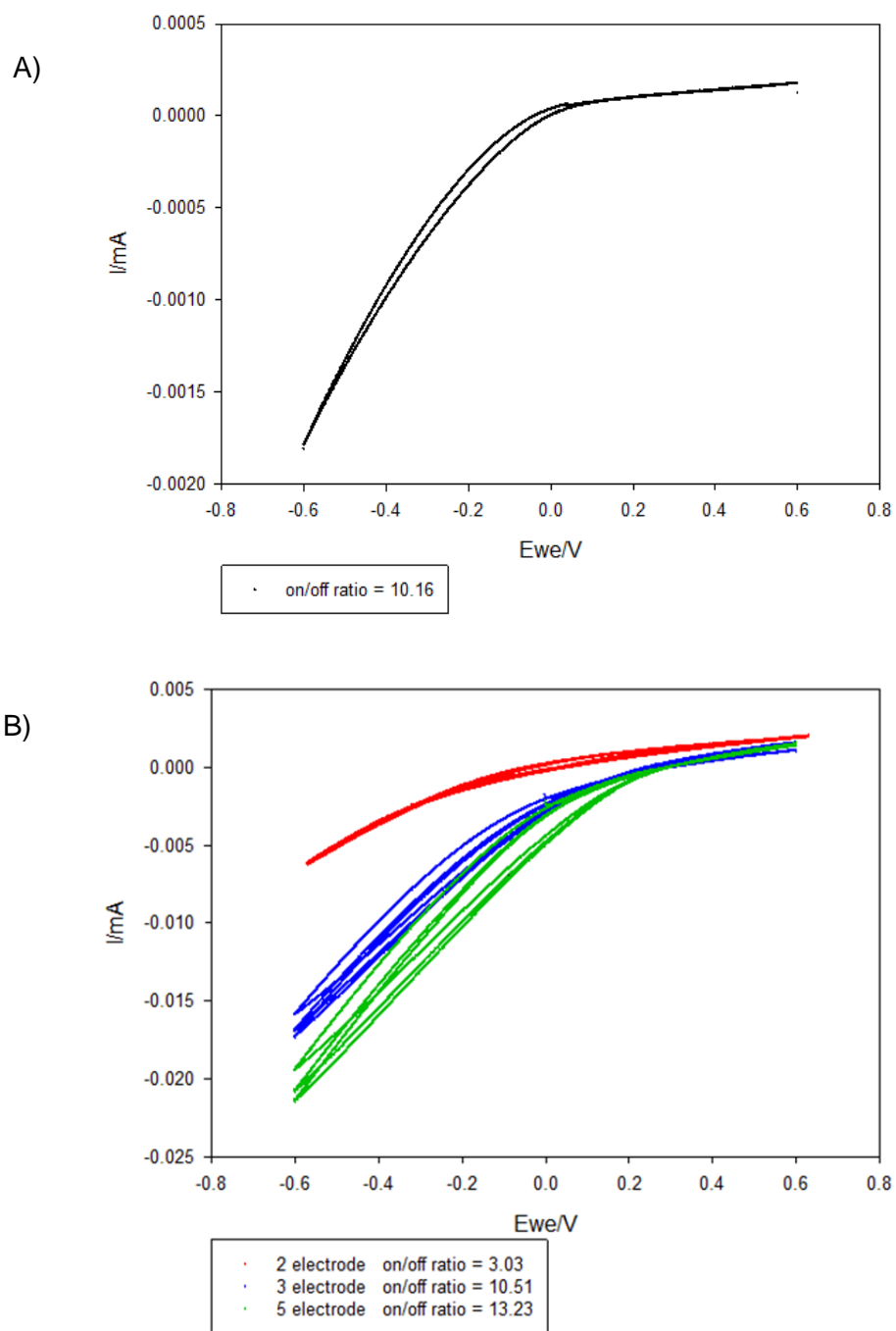
Figure 5. Demonstration of ionic current rectification using a 15 nm track-etched polycarbonate membrane (A) and the effects of using 2, 3, or 5 electrode systems on the on/off ratio (B).
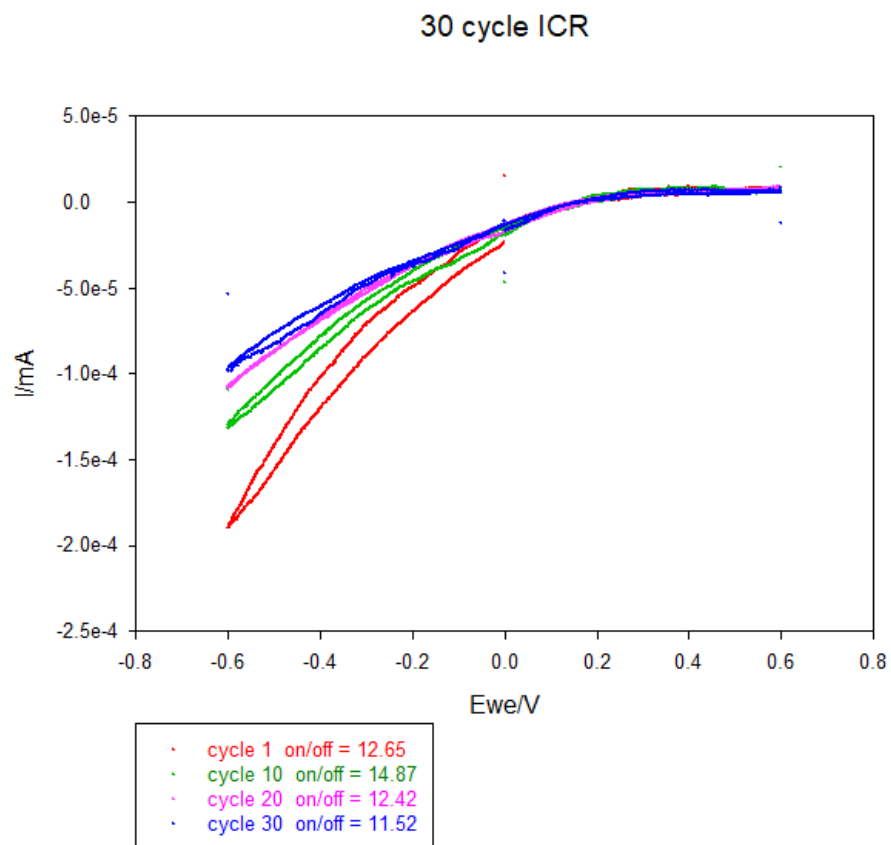
Figure 6. Demonstration of "cake layer" theory.

Drug Diffusion Data

Diffusion time (hr)	Total Sample (mL)	Sample Removed (mL)	[nicotine] (ppm)	Amount Permeated (µmol)	Removed [nicotine] (µmol)	Cum. (µmol)
0	6	1	0.0000	0.0000	0.0000	0.0000
8	6	1	6.923	0.2561	0.03356	0.2561
25	6	1	127.2	4.705	0.6166	4.738
32	6	1	91.31	3.377	0.4426	4.027
48	6	1	81.98	3.032	0.3974	4.125

Table 3. Data analysis of [nicotine] calculated using an external standard calibration curve into cumulative micromoles of nicotine diffused through a membrane with an on/off ratio of 10.51.
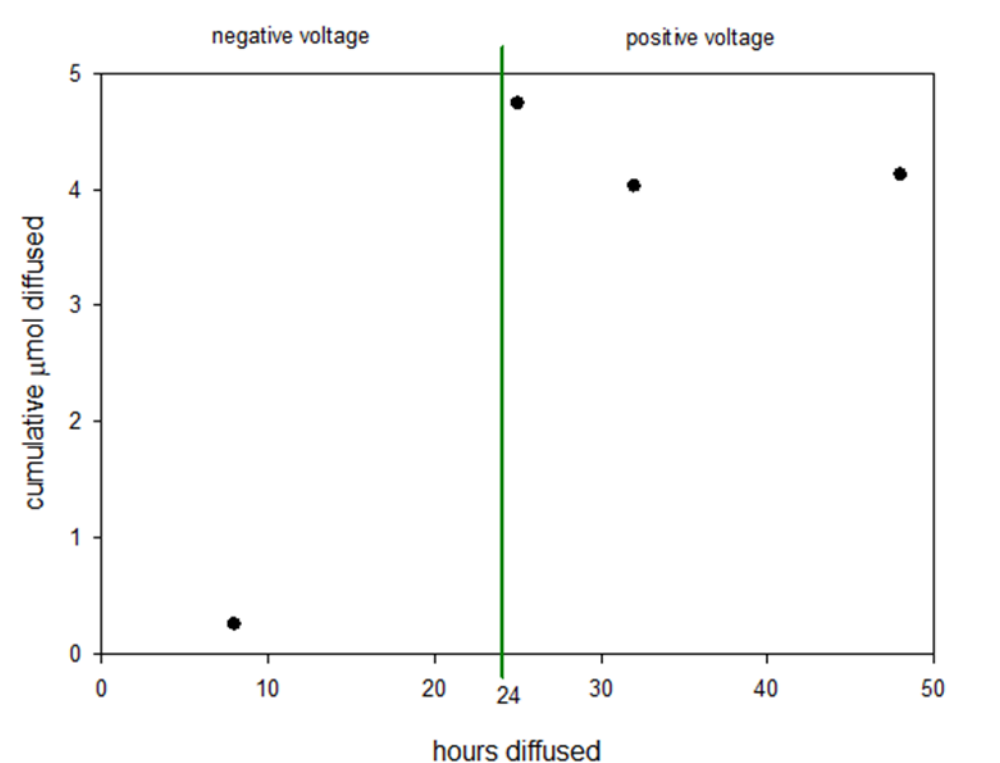
Figure 7. Graph of nicotine diffusion over time with cumulative micromoles of nicotine diffused shown on the y axis. Membrane on/off ratio = 10.51

Discussion

SNP synthesis. Agglomeration and precipitation of SNPs was a large obstacle to overcome. The amount of ammonia added to the formation reaction of non-functionalized SNPs as a catalyst controlled the final size of the particles, as did the time reacted.[15] Allowing the reaction to run longer than 24 hours resulted in particles that were too large. There is a limit to how large SNPs

can be while staying suspended in solution - at a point, their weight will be too heavy so that the force of gravity is larger than the electrostatic repulsion between NPs, resulting in precipitation of SNPs. It was also important that the SNPs were of small enough size to effectively block the nanopores in the membrane, seen in Figure 4, which were confirmed to be 15 nm by SEM imaging. Vigorous stirring during synthesis and reducing the reaction time to 8 hours for non-functionalized SNP synthesis alleviated this problem somewhat (see Table 2) considering that initial particle sizes were 200-300 nm in diameter. Functionalization of SNPs previously occurred overnight for approximately 15 hours. Literature search found that a reaction time of 20 minutes to 1 hour was sufficient and suggested sonication to prevent agglomeration issues.[16] Applying these techniques allowed us to reduce the size of functionalized SNPS from over 1000 nm to 212.35 nm in diameter as seen in Table 2. Stir bars were also added to the diffusion trials as a preventative measure. In future, there is still some improvements to be made, considering the target size of 50 nm and the %RSD values in Table 2.

Test Drugs. This study used aqueous buffer solutions as the primary medium and therefore had some challenges with drug solubility. The buffer solutions are necessary to protonate/deprotonate the SNPs and maintain their charge. They are also important to ensure functional groups on the test drugs are neutral. Ibuprofen was the first test drug used which was added to the pH 3 side of the U-tube to ensure that the OH group on the carboxylic acid was protonated. Unfortunately, our investigation found 100 ppm ibuprofen solutions would precipitate in the buffer and any ibuprofen diffused was below the detection limit of our HPLC method. Additions of ethanol were investigated to increase the solubility of ibuprofen and different proportions of buffer/ethanol solutions containing constant amounts of ibuprofen were analyzed

with HPLC to measure precipitation. Due to time constraints, ibuprofen was replaced with the much more water-soluble nicotine (16 g/L).

Proof of ICR Concept. When the voltage applied was positive, the SNPs blocked the membrane because the working electrode repelled the positively charged particles as the counter electrode repelled the negatively charged particles. When voltage applied was negative, particles attracted to their respective electrodes and away from the membrane allowing current to flow. This created a graph with a very small slope when positive voltage was applied and a very steep slope when negative voltage was applied. The ideal shape is represented in Figure 5 (A), which also contains the results of the multiple electrode systems test (B). The 2-, 3-, and 5-electrode systems showed that the on/off ratio for a given membrane increased with the increasing complexity of the electrode system (Figure 5 B). Adding the reference electrode to the 2-electrode system accounts for the IR drop due to the resistance of the membrane, and the two sensors added in the 5-electrode system do this with an even higher accuracy. Figure 6 shows that over 30 cycles, or roughly 2 hours, the current passing through the membrane decreased by almost half. This is expected because the cake layer increases L, the thickness of the membrane pore. The on/off ratio stays relatively stable throughout the cycles, which is a good sign against potential fouling for the 48-hour duration of the nicotine diffusion tests. The increase in L, however, can negatively impact the diffusion of nicotine, as will be discussed in the next section.

Fick's Law of Diffusion. The Fick's law experiment was designed to determine the porosity of the membrane due to the diffused nicotine being below the detection limit of the HPLC for nicotine quantification. This equation given below governs the passive diffusion of a compound through a membrane. *J* stands for the diffusion flux, *dC* is the concentration gradient, *L* is the

thickness of the pore, *D* is the diffusion coefficient of the molecule, n is the amount of moles of the molecule, *T* is time, and *A* is pore area.

$$J = D * \frac{dC}{L} = \frac{n}{T*A} \qquad T = \frac{n*L}{dC*D*A}$$

The unknown determined by the test was the total area, *A*, of the pores. This value was needed to initially determine *D*, the diffusion coefficient of nicotine in L/min*m. *L* was determined using SEM imaging. The value of *L* along with the internal KCl standard curve generated with ICP-MS were used to determine *A*. These standard values were then used to calculate n over a certain period of time with a certain donor concentration, and then *T*, the time it would take for the minimum amount of nicotine to diffuse through in order to be above the HPLC LOD. As we can see in the equation solved for time, the options to decrease the time are to increase the concentration gradient (*dC*) or area (*A*). This equation also implies that an increase in *L* will increase the time of diffusion. As explained in the above section, the formation of a cake layer of SNPs on the surface of the membrane increases *L* which will slow down the diffusion of a drug according to these equations. Large concentration gradients can combat this, but an issue arises with the water solubility of the drug. At most, 0.095 mL of nicotine can be added to the donor tube. Adding 80 mL, as was used in this experiment, produces a donor concentration of 13,467 ppm and still predicts 18.6 hours is needed to obtain a diffusion concentration of 8.5 ppm. Our study however showed this to not be true. Referring to Table 3, almost 7 ppm of nicotine was diffused in the first 8 hours of the test. This may be caused by using a different membrane in the diffusion study than was used in the Fick's Law experiment. The duct tape punctures are not uniform, therefore, the area of membrane exposed may differ for each one. There is also the fact that membrane porosity can differ between membranes. When considering the membrane SEM

image in Figure 4, potentially a membrane with a larger number of pores over the same cross-sectional image would be useful. To increase precision in the future, a Fick's Law test to determine *A* shall be performed on the membrane to take part in the diffusion study.

HPLC Method Development. The challenge with HPLC method development was reducing nicotine peak tailing, an issue seen in many papers using reversed phase HPLC or UFLC for nicotine detection and quantification.[17,18] Our method was originally based on the work of A. Alhusban[14] where they used triethylamine (TEA) as an additive to the aqueous mobile phase. Upon investigation of TEA, it was found that TEA is commonly used as a blocking agent for residual silanols found in reversed phase HPLC columns.[19] In reversed phase columns, the silica stationary phase is treated by attaching long alkyl chains so that the stationary phase has a greater affinity for nonpolar compounds. Not all surface silanol groups are modified like this, leaving a few polar surfaces that can affect retention time of compounds with polar or basic sites.[20] Nicotine contains pyridine and a tertiary amine, both basic sites. These sites on nicotine can be attracted by residual silanol groups, extending the retention time for a small portion of the nicotine present in the column. This was a major cause of peak tailing. A logical solution to prevent nicotine from being retained on residual silanol groups was to use a mobile phase containing a compound with a similar basic site, TEA being this compound. Literature suggested TEA concentrations of 30-50 mmol/L were most efficient, so concentration of TEA in water was increased from the original literature value of 0.1% to 0.5%.[19] This increase slightly improved the number of theoretical plates and visually produced a more Gaussian peak shape. Interestingly, the calibration curve using 0.1% TEA solvent had a better LOD, LOQ, and linearity constant than the calibration curve using 0.5% TEA. Eventually it was decided that the difference between the two concentrations was not significant enough and 0.1% TEA was used to produce the results in this paper.

Drug Diffusion Data. Time constraints and unexpected membrane fouling issues meant that only one set of diffusion data is able to be analyzed. The green line marked on Figure 7 represents the cutoff hour where voltage applied switches from negative to positive. Ideally, the 25-hour sample will be taken at 24 hours in the future. Figure 7 shows a large increase in moles diffused from hour 8 to hour 25, with the final diffusion concentration being 127.2 ppm (Table 3). Beyond this point, the diffused moles of nicotine decreased slightly, which was unexpected, but remained stable for the last two data points, proving that diffusion effectively stopped (see Table 3 and Figure 7). The decrease from hour 25 to hour 32 may be due to the fact that nicotine has the potential to become protonated in pH 3 buffer and thereby be bonded to silica particles through hydrogen bonding, leading to gradual loss with time. Alternatively, positive voltage may have pulled some protonated nicotine back across the membrane before it could be closed by the SNPs. When voltage is applied for long periods of time, a polarization of the buffer solution can occur. With this, it may take the SNPs some time to regain their strong charge and migrate back to the membrane pores. This may be alleviated in the future by adopting a high frequency pulsing method in place of the continuous application of a -0.6 or +0.6 V.

Conclusion and Future Work

This study has shown that the ICR phenomena created by the opening and closing of nanopores by SNPs has been optimized and has true potential for a drug delivery application. Future works include perfecting membrane fabrication to prevent leakage over the long diffusion experiment periods and gathering repeatable data. The potential formation of a SNP cake layer on the membrane has also been explored and can be further investigated by gathering SEM images of membranes before and after ICR tests. Application to other more water-soluble drugs would allow

a greater freedom to experiment with the Fick's Law parameters of concentration gradient relating

to time of diffusion. The 3-electrode system may also be applied to a drug diffusion test to verify

the 2-electrode data.

References

(1)   Watermann, A.; Brieger, J. Mesoporous Silica Nanoparticles as Drug Delivery Vehicles in Cancer. *Nanomaterials (Basel)* **2017**, *7* (7), 189. https://doi.org/10.3390/nano7070189.

(2)   Song, Y.; Li, Y.; Xu, Q.; Liu, Z. Mesoporous Silica Nanoparticles for Stimuli-Responsive Controlled Drug Delivery: Advances, Challenges, and Outlook. *Int J Nanomedicine* **2016**, *12*, 87–110. https://doi.org/10.2147/IJN.S117495.

(3)   Sadeghi, I.; Byrne, J.; Shakur, R.; Langer, R. Engineered Drug Delivery Devices to Address Global Health Challenges. *Journal of Controlled Release* **2021**, *331*, 503–514. https://doi.org/10.1016/j.jconrel.2021.01.035.

(4)   Tran, T.; Hernandez, M.; Patel, D.; Burns, E.; Peterman, V.; Wu, J. Controllable and Switchable Drug Delivery of Ibuprofen from Temperature Responsive Composite Nanofibers. *Nano Convergence* **2015**, *2* (1), 15. https://doi.org/10.1186/s40580-015-0047-5.

(5)   Kapoor, D. N.; Katare, O. P.; Dhawan, S. In Situ Forming Implant for Controlled Delivery of an Anti-HIV Fusion Inhibitor. *Int J Pharm* **2012**, *426* (1–2), 132–143. https://doi.org/10.1016/j.ijpharm.2012.01.005.

(6)   Smith, L.; Mosley, J.; Johnson, J.; Nasri, M. Probuphine (Buprenorphine) Subdermal Implants for the Treatment Of Opioid-Dependent Patients. *P T* **2017**, *42* (8), 505–508.

(7)   Wen, C.; Zeng, S.; Li, S.; Zhang, Z.; Zhang, S.-L. On Rectification of Ionic Current in Nanopores. *Anal. Chem* **2019**, *91*, 14597–14604.

(8)   Davis, S.; Macha, M.; Chernev, A.; Huang, D.; Radenovic, A.; Marion, S. Pressure-Induced Enlargement and Ionic Current Rectification in Symmetric Nanopores. *Nano Lett.* **2020**, *20*, 8089–8095.

(9)   Hou, X.; Dong, H.; Zhu, D.; Jiang, L. Fabrication of Stable Single Nanochannels with Controllable Ionic Rectification. *Small* **2010**, *6* (3), 361–365. https://doi.org/10.1002/smll.200901701.

(10)   Lin, C.-Y.; Yeh, L.-H.; Siwy, Z. S. Voltage-Induced Modulation of Ionic Concentrations and Ion Current Rectification in Mesopores with Highly Charged Pore Walls. *J. Phys. Chem. Lett.* **2018**, *9*, 393–398.

(11)   Tshwenya, L.; Marken, F.; Mathwig, K.; Arotiba, O. Switching Anionic and Cationic Semipermeability in Partially Hydrolyzed Polycarylonitrile: A PH-Tunable Ionic Rectifier. *ACS Appl. Mater. Interfaces* **2020**, *12*, 3214–3224.

(12)   Stöber, W.; Fink, A.; Bohn, E. Controlled Growth of Monodisperse Silica Spheres in the Micron Size Range. *Journal of Colloid and Interface Science* **1968**, *26* (1), 62–69. https://doi.org/10.1016/0021-9797(68)90272-5.

(13)   Pintro, C. "Controllable Drug Delivery Systems Using Nano-Porous Membranes and Functionalized Silica Nanoparticles." Presented at the 71st Southeastern Regional Meeting of the American Chemical Society, Savannah GA, USA, October 20-23, 2019.

(14)   Alhusban, A. A.; Ata, S. A. Simple HPLC Method for Rapid Quantification of Nicotine Content in E-Cigarettes Liquids. *Acta Chromatographica* **2020**, *33* (3), 302–307. https://doi.org/10.1556/1326.2020.00832.

(15)   Greasley, S. L.; Page, S. J.; Sirovica, S.; Chen, S.; Martin, R. A.; Riveiro, A.; Hanna, J. V.; Porter, A. E.; Jones, J. R. Controlling Particle Size in the Stöber Process and Incorporation of Calcium. *J. Colloid Interface Sci.* **2016**, *469*, 213–223. https://doi.org/10.1016/j.jcis.2016.01.065.

(16)   Acres, R. G.; Ellis, A. V.; Alvino, J.; Lenahan, C. E.; Khodakov, D. A.; Metha, G. F.; Andersson, G. G. Molecular Structure of 3-Aminopropyltriethoxysilane Layers Formed on Silanol-Terminated Silicon Surfaces. *J. Phys. Chem. C* **2012**, *116* (10), 6289–6297.

https://doi.org/10.1021/jp212056s.

(17)   Ayoub, B. M.; Mohamady, S.; Hendy, M. S.; Elmazar, M. M. Enhanced Chromatographic Determination of Nicotine in Human Plasma: Applied to Human Volunteers. *Int J Biomed Sci* **2015**, *11* (4), 185–189.

(18)   Tsuji, M.; Mori, Y.; Kanda, H.; Ito, T.; Hidaka, T.; Kakamu, T.; Kumagai, T.; Hayakawa, T.; Osaki, Y.; Fukushima, T. Development of Simple HPLC/UV with a Column-Switching Method for the Determination of Nicotine and Cotinine in Hair Samples. *Health* **2013**, *5* (No.4). https://doi.org/10.4236/health.2013.54091.

(19)   Law, B. Pharmaceuticals: Basic Drugs: Liquid Chromatography. In *Encyclopedia of Separation Science*; 2000; pp 3701–3708.

(20)   Bocian, S.; Buszewski, B. Residual Silanols at Reversed-Phase Silica in HPLC - a Contribution for a Better Understanding. *J. Sep. Sci* **2012**, *35*, 1191–1200.